Angiopoietin-1 protects against endotoxin-induced neonatal lung injury and alveolar simplification in mice.

Umar Salimi[1,*],

Heather L. Menden[2,3,*],

Sherry M. Mabry[2,3],

Sheng Xia[2,3],

Venkatesh Sampath[2,3,#]

[1]Division of Pediatric Critical Care, Department of Pediatrics, Children's Mercy Kansas City, Kansas City, MO

[2]Division of Neonatology, Department of Pediatrics, Children's Mercy Kansas City, Kansas City, MO

[3]Neonatal Diseases Research Program, Children's Mercy Research Institute, Kansas City, Kansas City, MO

Abstract

Background—Sepsis in premature newborns is a risk factor for bronchopulmonary dysplasia (BPD), but underlying mechanisms of lung injury remain unclear. Aberrant expression of endothelial cell (EC) angiopoietin 2 (ANGPT2) disrupts angiopoietin 1 (ANGPT1)/TIE2-mediated endothelial quiescence, and is implicated in sepsis-induced acute respiratory distress syndrome in adults. We hypothesized that recombinant ANGPT1 will mitigate sepsis-induced ANGPT2 expression, inflammation, acute lung injury (ALI), and alveolar remodeling in the saccular lung.

Methods—Effects of recombinant ANGPT1 on lipopolysaccharide (LPS)-induced endothelial inflammation were evaluated in human pulmonary microvascular endothelial cells (HPMEC). ALI and long-term alveolar remodeling were assessed in newborn mice exposed to intraperitoneal LPS and recombinant ANGPT1 pretreatment.

#Corresponding author information: Venkatesh Sampath, MD, Professor of Pediatrics, 2401 Gillham Rd, Division of Neonatology, Kansas City, MO 64108, Ph: (816) 234-3591, Fax: (816) 302-9887, vsampath@cmh.edu.
*Author Contributions:
Conception and design: VS, US, HM
Data collection: US, HM, SX, SM
Analysis and interpretation: VS, US, HM, SM, SX
Drafting and editing the manuscript: US wrote first draft of manuscript, VS and HM edited. VS approved final version for submission.

Results—LPS dephosphorylated EC TIE2 in association with increased ANGPT2 *in vivo* and *in vitro*. ANGPT1 suppressed LPS and ANGPT2-induced EC inflammation in HPMEC. Neonatal mice treated with LPS had increased lung cytokine expression, neutrophilic influx, and cellular apoptosis. ANGPT1 pre-treatment suppressed LPS-induced lung Toll-like receptor signaling, inflammation, and ALI. LPS-induced acute increases in metalloproteinase 9 expression and elastic fiber breaks, as well as a long-term decrease in radial alveolar counts, were mitigated by ANGPT1.

Conclusions—In an experimental model of sepsis-induced BPD, ANGPT1 preserved endothelial quiescence, inhibited ALI, and suppressed alveolar simplification.

Introduction

Inflammation in the saccular lung disrupts its developmental program and contributes to bronchopulmonary dysplasia (BPD) in preterm neonates, a lifelong condition of impaired tolerance to activity and susceptibility to severe episodic respiratory illness (1,2). Postnatal insults such as sepsis, hyperoxia, and ventilator-induced lung injury in premature neonates inhibit secondary septation and result in alveolar simplification (2,3). In the last decade, sepsis has emerged as a prominent risk factor for BPD (4). During gram-negative sepsis, lipopolysaccharide (LPS), a component of the bacterial cell wall, binds to Toll-like receptor 4 (TLR4) to induce systemic and pulmonary inflammation (5). A relationship between TLR signaling, gram-negative lung infection, and alveolar remodeling was previously characterized in mice (6), and more recently, we demonstrated that a single intraperitoneal dose of endotoxin (LPS) in newborn mice induces alveolar simplification akin to BPD in preterm neonates (7). In this sterile sepsis model, we noted prominent lung endothelial cell (EC) immune activation contributing to neutrophil influx and acute lung injury (ALI), also observed in gram-negative sepsis in neonates (7,8). Vascular growth factors such as angiopoietins are potent regulators of endothelial permeability and inflammation (9,10). Whether modulation of angiopoietin signaling during neonatal sepsis suppresses ALI and preserves alveolar development remains unknown and is investigated herein.

Angiopoietins, ligands of the endothelial receptor tyrosine kinase TIE2, have increasingly been implicated in vascular inflammatory disease (9,10). During endothelial quiescence, mesenchymal cells secrete Angiopoietin 1 (ANGPT1), which strongly agonizes TIE2 by stimulating receptor autophosphorylation (11). Phosphorylated TIE2 localizes to cell-cell junctions and upregulates VE-cadherin complexes to support endothelial barrier function (10). In addition, activated TIE2 promotes EC survival, suppresses inflammation, and inhibits transcription of the vessel destabilizing factor Angiopoietin 2 (ANGPT2) (12,13). In the presence of infection however, ANGPT2 released from endothelial intracellular storage granules competitively inhibits ANGPT1-TIE2 interactions, dephosphorylating TIE2 and disturbing EC quiescence (14,15). Increased endothelial permeability and responsiveness to pro-inflammatory cytokines result (16). Septic premature infants demonstrate elevated bloodstream ANGPT2/ANGPT1 ratios (17), but the pathophysiologic significance of increased EC ANGPT2 relative to ANGPT1 in sepsis-induced lung injury has been only explored in adult experimental models (16,18). During lung development, the precise spatiotemporal expression of ANGPT1 and ANGPT2 in the saccular lungs of mice is

a crucial determinant of pulmonary vascularization and alveolar formation (19). Thus, perturbation of ANGPT1-TIE2 axis with sepsis in the developing lung has implications for aberrant alveolarization in BPD warranting further investigation.

Acute lung injury is characterized by neutrophilic influx, cell death, pulmonary edema (20), and protease-mediated tissue degradation, which in the developing lung promote alveolar remodeling (1,2). While the pathogenic mechanisms of ALI remain poorly defined in newborns, work in our lab and others suggest that the pulmonary endothelium factors prominently by priming neutrophil infiltration (8,21). Tempering pulmonary EC immune activation by ANGPT1 agonism or ANGPT2 antagonism represent attractive strategies to inhibit sepsis-induced ALI, and both approaches have shown potential therapeutic benefit in adult animal and human studies (22,23). Therefore, we hypothesized that exogenous ANGPT1 would mitigate dysregulation of the ANGPT1-TIE2 axis induced by elevated ANGPT2 in neonatal sepsis, alleviating ALI and alveolar remodeling. We demonstrate that recombinant ANGPT1 suppresses LPS-induced endothelial inflammation in primary fetal lung EC and ameliorates alveolar simplification following systemic LPS exposure in a pre-clinical model of BPD. Further, we show that these effects occur via the inhibition of ANGPT2 influx, TIE2 dephosphorylation, and pro-inflammatory TLR4 signaling.

Materials and Methods

Ethical Approval and Animal Model:

Care of mice before and during the experimental procedures was conducted in accordance with policies at the University of Missouri-Kansas City Lab Animal Resource Center (Protocol 1510–02). All protocols had prior approval from the University of Missouri-Kansas City Institutional Animal Care and Use Committee. C57BL/6 mice were obtained from Charles River (Burlington, MA). All animal experiments were performed using mouse pups between day of life 6 and 15. Lipopolysaccharide (LPS, 2mg/kg) was given intraperitoneally (i.p), with controls receiving sterile saline (Sigma, St. Louis, MO). Recombinant mouse ANGPT1 (rmANGPT1, R&D Systems, Minneapolis, MN) was injected i.p at 1.0μg per pup 2h prior to LPS, and for long-term study an additional dose was administered 72h following LPS. Pups were euthanized and lungs harvested at 24 and 196h post-LPS injections as described previously (8).

Cell Culture and Reagents:

Human primary pulmonary microvascular endothelial cells (HPMEC, ScienCell, Carlsbad, CA) derived from fetal lung tissue (gestational age 18–19 weeks, 2 female lots and 1 male lot), were used according to manufacturer's instructions (8). HPMEC are representative of capillaries. E. Coli Ultrapure 055:B5 LPS (100ng/mL) was purchased from Invivogen (San Diego, CA). Recombinant human ANGPT1 (rhANGPT1, 200ng/mL) and recombinant human ANGPT2 (rhANGPT2, 25ng/mL) were purchased from R&D Systems. For experiments with rhANGPT1 *in vitro*, cells were pre-treated for 1h prior to the addition of LPS or rhANGPT2.

Hematoxylin and Eosin Staining to Assess Lung Development in Mice:

15-day-old mice were euthanized 196h after i.p. LPS injection, having received rmANGPT1 i.p. 2 hours prior to and 72 hours following LPS. Lungs were inflated with 300μL of formalin over 30 seconds under constant pressure through a 24g angiocath. Lungs were formalin-fixed, processed into slides, and stained with H&E, then assessed for radial alveolar count (RAC) and mean linear intercepts (MLI) on an Olympus BX60 microscope using previously described methods (26,27). A minimum of 5 fields per mouse were assessed for RAC and MLI, and the averages used for quantifications.

Data Analysis:

Data are presented as mean ± SD. For HPMEC experiments, quantitative data are representative of 3–6 independent experiments. For animal experiments, 5–8 mice were used for each experimental group. When data was further analyzed for sex-based differences, there were 3 experiments per condition. Data were assessed for Gaussian distribution (i.e. normality) using the D'Agostino-Pearson omnibus test. If normally distributed, then a one-way ANOVA with a post-hoc Tukey's test was used. If data did not meet Gaussian assumptions, a Kruskal-Wallis test with Dunn's correction or a Mann-Whitney U test was used. A p-value <0.05 was considered significant. Statistical analysis was done using GraphPad Prism 8.0.2 (San Diego, CA).

Additional methods: Available in the online supplement (https://www.nature.com/pr/)

Results

Recombinant ANGPT1 (rhANGPT1) inhibits LPS-induced TIE2 dephosphorylation, NF-κB activation, and cytokine expression in human pulmonary microvascular endothelial cells (HPMEC):

We investigated whether endotoxin (LPS) induces TIE2 dephosphorylation, indicating loss of EC quiescence, using HPMEC *in vitro*. LPS induced pTIE2 dephosphorylation by western blot of HPMEC lysates (Fig. 1a,1b), and the addition of rhANGPT1 rescued LPS-induced TIE2 dephosphorylation. rhANGPT1 was evaluated at 3 different doses and was most efficacious at 200 ng/mL, which was subsequently used for all *in vitro* experiments. Evaluation of LPS-induced TIE2 protein phosphorylation by HPMEC sex did not reveal significant differences, and recombinant rhANGPT1 rescue was similar between males and females (Supplemental Figure S1 (online)). We further validated rhANGPT1 rescue of LPS-induced pTIE2 dephosphorylation by immunofluorescence, which revealed loss of pTIE2 fluorescence after LPS treatment at 18h, and preservation in HPMEC pre-treated with rhANGPT1 (Fig. 1c). We next examined the effect of rhANGPT1 on LPS-induced pro-inflammatory EC signaling. LPS induced *IL-8* and *IL-1β* mRNA expression robustly in HPMEC (p<0.01, n=3/sex), and this was inhibited with rhANGPT1 pre-treatment in a dose-dependent manner (Fig. 1d,1e). Intercellular adhesion molecule 1 (ICAM1), a key marker of endothelial activation that facilitates neutrophil influx *in vivo,* was strongly induced at the RNA and protein level by LPS and suppressed by rhANGPT1 (Fig. 1f, 1g, 1h). The effects of rhANGPT1 on LPS-induced pro-inflammatory signaling was not sex-dependent (Fig. 1d, 1e) (n=3/sex). We found that LPS-mediated phosphorylation of

p65 (RELA, component of pro-inflammatory transcription factor NF-κB), a marker of NF-κB activation, was suppressed with rhANGPT1 (Fig. 1g, 1h). These data suggest that rhANGPT1 inhibits LPS-induced NF-κB activation and cytokine expression in HPMEC by restoring TIE2 phosphorylation. HPMEC viability was tested by trypan blue assay. EC viability significantly decreased with LPS treatment (Fig. 1i) but was improved by addition of rhANGPT1 in a dose-dependent manner. On exposure to rhANGPT1 alone, there was a nonsignificant increase in cell viability compared to control.

rhANGPT1 antagonizes rhANGPT2-mediated cytokine expression and autocrine positive feedback loop in HPMEC:

We next delineated the relationship between LPS, ANGPT2, and ANGPT1 during HPMEC inflammation. LPS increased *ANGPT2* and *TIE2* RNA expression but did not induce *ANGPT1* RNA (Fig. 2a). We posited that ANGPT2 induced by LPS can induce inflammation in HPMEC. To evaluate this, we treated HPMEC with recombinant ANGPT2 (rhANGPT2, 25ng/ml). rhANGPT2 induced early (6 h) expression of pro-inflammatory cytokines (Fig. 2b). Co-stimulation with rhANGPT1 suppressed rhANGPT2-induced *ICAM1*, *IL-8*, *IL-1β,* and *TNF-α* gene expression (Fig. 2c).

We next determined whether ANGPT2 can induce self-expression in HPMEC and noted that rhANGPT2 (25ng/ml) induced *ANGPT2* gene expression at 18h (Fig. 2d). rhANGPT2-induced *ANGPT2* expression was strongly suppressed by rhANGPT1 (Fig. 2d). rhANGPT1 did not induce *ANGPT2* expression. Further, we noted that LPS-mediated ANGPT2 protein was inhibited with rhANGPT1 co-treatment (Fig. 2e, 2f). LPS did not induce TIE2 protein significantly in HPMEC (Fig. 1b, 1c). These data suggest that LPS induces ANGPT2 expression in HPMEC, and that ANGPT2 induces cytokines and its own autocrine expression. Further, rhANGPT1 can inhibit both LPS and ANGPT2-induced cytokine expression in HPMEC. Our data demonstrate that rhANGPT1 can mitigate LPS-induced TIE2 dephosphorylation along with the pro-inflammatory effects of NF-κB and ANGPT2 signaling in lung EC.

Recombinant ANGPT1 inhibits LPS-mediated TIE2 dephosphorylation, ANGPT2 expression, inflammatory cytokines, and markers of EC immune activation in a mouse model of neonatal sepsis:

To investigate our findings *in vivo*, we pursued studies in a pre-clinical model of neonatal sepsis our lab developed (7). LPS (2mg/kg, i.p.) induced pTIE2^{Y992} dephosphorylation in lung EC, as shown by immunofluorescence (Fig. 3a). As in HPMEC, LPS induced *Angpt2*, but not *Angpt1,* RNA expression in whole lung (Fig. 3c). We initially tested dosing strategies of recombinant mouse ANGPT1 (rmANGPT1) as it has not been studied in neonatal mice (Supplemental Figure S2 (online)). We identified a single i.p. dose of 1μg as therapeutic, based on comparisons between 0.1ug i.p, 0.3ug i.p (each two doses given 12h apart), 0.6ug, and 1.0ug i.p (each one dose only), starting 2h before LPS administration and using lung ANGPT2 protein and cytokine expression as end points (Supplemental Figure S2 (online)). Subsequent studies were done with 1μg i.p. of rmANGPT1.

Pre-treatment with rmANGPT1 (2h) suppressed LPS-induced TIE2 dephosphorylation (Fig. 3a, 3b) as in HPMEC, in parallel with decreased ANGPT2 mRNA and protein (Fig. 3c, 3d, 3e). LPS robustly induced lung expression of *Tnf-a, Kc* (mouse equivalent of *IL-8*), and *Il-1β*. The effect was suppressed with rmANGPT1 (Fig. 3f). Expression of intercellular adhesion molecules promotes EC and neutrophil/macrophage interactions that facilitate lung infiltration. LPS-induced expression of adhesion molecules *Icam1* and *Sele* (E-selectin) at 24h was inhibited by pre-treatment with rmANGPT1 (Fig. 3f). Lung ICAM1 protein, strongly induced by systemic LPS, was also suppressed by rmANGPT1 (Fig. 3g, 3h). These data suggest that LPS-induced TIE2 dephosphorylation and ANGPT2 expression promote increased cytokine and adhesion molecule expression, which is attenuated by rmANGPT1.

rmANGPT1 inhibits lung vascular permeability, neutrophil influx, and cell death in a preclinical model of neonatal sepsis:

We next examined elements of ALI in our mouse model. Bronchoalveolar lavage (BAL) showed that the total cell count increased >2.2-fold after LPS and was suppressed >60% in mice treated with rmANGPT1 (fig. 4a). The LPS-induced increase in lung cell count was predominantly due to increased neutrophil influx and was almost completely abolished with rmANGPT1 pre-treatment (Fig. 4b). BAL albumin concentration increased >2-fold with systemic LPS and was attenuated by rmANGPT1, indicating decreased vascular leakiness (Fig. 4c). Sex-based differences in systemic LPS-induced lung injury were evaluated for BAL data (Fig. 4d, 4e) and revealed no significant differences between male and female mice (n=3–5/sex/condition). We next investigated whether systemic LPS caused lung cell death by apoptosis, characteristic of ALI. Lung apoptosis, quantified by TUNEL assay, increased from <0.5% in controls to 6% in LPS-treated pups. LPS-induced apoptosis was suppressed in pups that were treated with rmANGPT1 (Fig. 4d, 4e). These data demonstrate that LPS-induced ALI in the developing lung is ameliorated by rmANGPT1.

rmANGPT1 inhibits Toll-like Receptor (TLR) signaling and suppresses markers of early alveolar remodeling induced by LPS:

Activation of TLR signaling in the lung drives NF-κB-dependent pro-inflammatory signaling and matrix digestion (6,19). We therefore examined the effect of rmANGPT1 on canonical TLR signaling in the lung. LPS induced phosphorylation of inhibitor of nuclear factor kappa-B kinase subunit beta (IKKβ) as well as MAPK (p38) at 24h, indicating activation of canonical TLR signaling (Fig. 5a). We also noted that p65 phosphorylation was induced with LPS (Fig. 5b), suggesting activation of NF-κB. LPS-mediated phosphorylation of pIKKβ, p38, and p65 was attenuated with rmANGPT1 pre-treatment (Fig. 5a, 5b, 5c), supporting negative regulation of TLR-dependent canonical signaling by rmANGPT1.

ALI is associated with activation of proteases that result in lung matrix digestion in the acute phase, and alveolar remodeling in the chronic phase. We examined expression of matrix metalloproteinase 9 (MMP9), and the tissue inhibitor of metalloproteinase 1 (TIMP1), an antiprotease in the lung. LPS induced gene expression of both *Mmp9* and *Timp1*, with *Mmp9* more strongly induced (Fig. 5d). rmANGPT1 pretreatment suppressed LPS-induced *Mmp9*, but not *Timp1* RNA expression (Fig. 5d). Destruction of the elastic fiber architecture is a key event in sepsis-induced ALI, and we quantified this in alveoli, excluding blood

vessels and conducting airways. We noted that the continuous, homogenous elastic fiber staining of alveoli found in controls was disrupted in pups treated with LPS (Fig. 5e). rmANGPT1 partially rescued LPS-induced alveolar elastic fiber breaks (Fig. 5e, 5f).

rmANGPT1 rescues lung EC population and alveolar remodeling induced by LPS:

We and others have shown that decreases in the lung EC population is a hallmark of rodent and human BPD (8,28,29). We evaluated alveolar remodeling and EC population on mouse day of life 15, which represents the mid-alveolar phase, after LPS treatment on day of life 7 and rmANGPT1 on days 7 and 10. There was a notable decrease in the population of cells positive for the EC nuclear marker ETS-related gene (ERG-Red (nucleus); DAPI-blue) after LPS treatment (Fig. 6a). rmANGPT1 rescued LPS-induced decreases in ERG+ cell numbers, indicative of preserved lung EC population (Fig. 6a, 6b). Alveolar simplification is the sine qua non of BPD in human and pre-clinical models of BPD. Lung morphometry revealed that LPS induced alveolar simplification (Fig. 6c), evident by decreased radial alveolar counts (RAC) and increased mean linear intercepts (MLI) on day of life 15 (Fig. 6d, 6e). Decreased RAC and increased MLI seen with LPS were >60% rescued in mice treated on days of life 7 and 10 with rmANGPT1 (Fig. 6d, 6e). There were no significant sex-based differences (n=3–5/sex/condition) in lung morphometry (Fig. 6f, 6g). These data demonstrate that rmANGPT1, by suppressing ALI induced by LPS, rescues the murine chronic alveolar remodeling phenotype akin to BPD in human infants.

Discussion

The Angiopoietin-TIE2 axis regulates pulmonary vascular homeostasis, yet its role in neonatal sepsis-induced acute lung injury and alveolar remodeling remains understudied. Using fetal HPMEC and newborn mice, we demonstrate that constitutive TIE2 receptor phosphorylation is lost in association with elevated ANGPT2 during sepsis-induced ALI in the developing lung, and that recombinant ANGPT1 mitigates these effects. Recombinant ANGPT1 suppressed LPS-induced acute pulmonary inflammation, alveolar-capillary permeability, apoptosis, and matrix degradation in newborn mice in parallel with attenuation of canonical TLR signaling. Over the long term, recombinant ANGPT1 protected against alveolar simplification mimicking BPD in a sex-independent manner. Our findings indicate that the angiopoietin-TIE2 axis regulates sepsis-induced endothelial activation in the developing lung, and that exogenous ANGPT1 can be protective in this setting. The potential for ANGPT1 agonism to mitigate BPD in preterm infants merits further investigation.

We observed an antagonistic relationship between ANGPT1 and ANGPT2, with opposing effects on inflammation mediated through the EC receptor TIE2. Using an *in vitro* model of fetal HPMEC, we demonstrate that LPS dephosphorylates TIE2, while the addition of the TIE2 agonist ANGPT1 maintains receptor phosphorylation, suppresses cytokine and adhesion molecule expression, and preserves cell viability in a dose-dependent, and sex-independent manner. Anti-inflammatory effects appeared to be, in part, facilitated by NF-κB inhibition, which is consistent with prior studies demonstrating that the stabilization of TIE2 phosphorylation by ANGPT1 promotes A20 binding inhibitor of NF-κB 2 (ABIN-2)-

dependent NF-κB suppression (11,12). ANGPT2 was notably elevated in response to LPS along with pro-inflammatory cytokines, as observed previously (18,30). With direct rhANGPT2 stimulation of HPMEC, we noted an acute increase in *ICAM1* and cytokine expression (*TNF-a, IL-1β, IL-8*) in the absence of LPS, suggesting that ANGPT2 induced by LPS further propagates inflammation. rhANGPT2 also induced its own expression, consistent with previous observations (15). rhANGPT1 inhibits both rhANGPT2-mediated inflammation and autocrine self-expression. In summary, these data specify multiple mechanisms by which ANGPT1 inhibits LPS-induced inflammation and maintains TIE2-dependent EC quiescence.

Angiopoietin 1 therapy has shown promising effects on ALI and mortality in adult models of sepsis (22,31,32). Here we show that pretreatment of newborn mice with rmANGPT1 attenuates LPS-induced lung cytokine and adhesion molecule expression, pulmonary capillary permeability, neutrophil influx, and lung cellular apoptosis. Prior studies of angiopoietin 1 for LPS-induced adult ALI evaluated transgenic pulmonary overexpression of ANGPT1 (31,32), but we administered recombinant ANGPT1 to investigate the translatable potential of ANGPT1 in neonatal sepsis-induced ALI. Similar to our findings, Sascha et al. observed reduced lung adhesion molecule expression, neutrophil infiltration, and injury in an adult murine cecal ligation and puncture sepsis model using recombinant ANGPT1 (33). On the other hand, McCarter et al. and Hegeman et al. failed to demonstrate similar effects with systemic ANGPT1 in rodent models of inhaled LPS and ventilator-induced ALI, respectively (31,34). Lack of efficacy in models of direct pulmonary injury may relate to imprecise targeting of the endothelial angiopoietin-TIE2 axis, which we achieved using systemic LPS delivery to mimic sepsis. Our finding of pulmonary TIE2 phosphorylation following i.p. recombinant ANGPT1 administration importantly demonstrates lung activity for this systemic treatment. However, it is additionally plausible that systemic ANGPT1 counters pulmonary inflammation by promoting anti-inflammatory mediators (e.g. IL-4, IL-10) distal to the lung, which deserves investigation. While we used prophylactic ANGPT1 dosing, other researchers have shown rescue of adult rodents from sepsis-induced ALI (33,35). Investigating rmANGPT1 as a rescue strategy in our neonatal model will be an important translational step.

Angiopoietin 1 binds the EC surface tyrosine kinase TIE2 as its principle receptor, maintaining endothelial quiescence by phosphorylating TIE2 (11–13). Here we show that with LPS exposure, pulmonary ANGPT2 is elevated while TIE2 is dephosphorylated in lung EC, implying loss of endothelial quiescence. The ability of rmANGPT1 to maintain TIE2 phosphorylation, suppress ANGPT2 expression, and suppress LPS-induced lung inflammation suggests that the pathologic imbalance of ANGPT2:ANGPT1 observed in adult sepsis studies extends to our neonatal sepsis model. These findings are consistent with those of McCarter et al., who found higher phosphorylated TIE2 protein in rats receiving ANGPT1 gene therapy for LPS-induced ALI (31). To further characterize the anti-inflammatory mechanisms of ANGPT1-TIE2 agonism, we explored canonical pulmonary LPS-TLR4 signaling and found that both the IKKβ/NF-κB and MAP Kinase (p38) pathways were curbed with our pretreatment. We postulate that TIE2-mediated NF-κB inhibition via ABIN-2 suppresses IL-1β and other cytokines that signal through the Interleukin 1 receptor to mediate Toll/Interleukin-1 receptor (TIR) homology domain-dependent MAPK and IKKβ

signaling (5). Though inhibition of constitutive NF-κB activity in the developing lung stunts alveolarization by impairing VEGF-mediated pulmonary angiogenesis (36), Mckenna et al. demonstrated that administration of the IKK inhibitor BAY during LPS exposure can selectively target IκBβ/NF-κB-mediated transcription of pro-inflammatory genes, including the lung injury mediator IL-1β, without impairing developmentally beneficial IκBα signaling (37). The latter data are congruent with our finding that rmANGPT1-mediated inhibition of transient LPS-induced NF-κB, IKKβ, and p38 activation benefits lung development by countering inflammation and ensuing neonatal lung injury. While our data support TIE2's role in neonatal sepsis-induced ALI, one limitation is that we did not examine TIE2-independent, angiopoietin interactions with alpha5 integrins, which can also regulate EC inflammation (38).

Studies in premature infants describe low airway ANGPT1 and elevated ANGPT2 levels early on in those who develop BPD (39,40). Further, increases in MMP9, without corresponding elevations in inhibitors such as TIMP1 are observed in lung fluid from preterm infants who subsequently develop BPD (41). In our model, we observed an acute breakdown in alveolar elastic fibers and an elevated MMP9/TIMP1 ratio. rmANGPT1 suppressed the deleterious effects of LPS on matrix modeling and protease/antiprotease imbalance. The lung EC population, marked by ERG, was depleted with LPS and restored with rmANGPT1. The decrease in EC population with LPS is likely a consequence of alveolar simplification. This is supported by our data showing decreased RAC and increased MLI in pups treated with LPS, consistent with previous studies (7,8,42), with rescue by rmANGPT1 treatment. Interestingly, mice genetically bred by Hato et al. to overexpress ANGPT1 in a lung-specific fashion developed dysmorphic pulmonary vasculature and alveolar simplification (19). This study suggests that constitutive ANGPT1 overexpression inhibits lung vascular development, potentially by disrupting the typical sequence of angiogenic events. On the other hand, our control data shows that limited ANGPT1 agonism in the context of excessive EC ANGPT2 activity has no long-term lung morphologic effects. Bhandari et al. showed that hyperoxia-mediated alveolar remodeling is suppressed in *Angpt2*–/– mice (43), while Liang et al. saw decreased ANGPT1 levels associated with aberrant pulmonary vascular development in hyperoxia-exposed rat pups (44). The latter posited a contribution of impaired ANGPT1-TIE2 signaling to BPD pathogenesis, although TIE2 phosphorylation was not probed. While our data shows a role for exogenous ANGPT1 rescue of TIE2 phosphorylation in the setting of sepsis, careful consideration of timing, dose, and duration is required to avoid deleterious effects of persistent ANGPT1-TIE2 agonism in the developing lung. Studies using *Angpt2*–/– mice were not pursued because of the presence of severe pulmonary lymphatic defects and our goal of identifying translatable therapies.

In conclusion, this is one of the first studies to demonstrate that recombinant ANGPT1 protects against sepsis-induced alveolar remodeling in newborn mice by maintaining endothelial quiescence. Using both *in vivo* and *in vitro* models, we reveal the significance of preserving EC TIE2 phosphorylation and suppressing ANGPT2 in mitigating endotoxin-mediated EC inflammation, ALI, and alveolar simplification. Suppression of pro-inflammatory TLR signaling, and its ready availability, make recombinant ANGPT1 an appealing adjunct therapy during postnatal sepsis, a major risk factor for BPD. Key steps

toward clinical translation will be application to non-sterile models of lung inflammation as well as rescue dosing strategies. Direct inhibition of ANGPT2 using neutralizing antibodies represents another potential approach. This study highlights the relevance of preserving ANGPT1-TIE2 mediated EC quiescence and suppressing ANGPT2 signaling in the prevention of sepsis-induced ALI and experimental BPD.

Supplementary Material

Refer to Web version on PubMed Central for supplementary material.

ACKNOWLEDGEMENTS

REFERENCES

1. Ogden BE, Murphy S, Saunders GC, Johnson JD Lung lavage of newborns with respiratory distress syndrome: Prolonged neutrophil influx is associated with bronchopulmonary dysplasia. Chest. 83(5 Suppl), 31S–33S (1983). [PubMed: 6601571]

2. Shahzad T, Radajewski S, Chao CM, Bellusci S, Ehrhardt H. Pathogenesis of bronchopulmonary dysplasia: when inflammation meets organ development. Mol Cell Pediatr. 3(1), 23 (2016). [PubMed: 27357257]

3. Coalson JJ Pathology of bronchopulmonary dysplasia. Semin Perinatol. 30, 179–184 (2006). [PubMed: 16860157]

4. Shah J, Jefferies AL, Yoon EW, Lee SK, Shah PS Canadian Neonatal Network. Risk factors and outcomes of late-onset bacterial sepsis in preterm neonates born at 32 weeks' gestation. Am J Perinatol 32, 675–682 (2015). [PubMed: 25486288]

5. Anderson KV Toll signaling pathways in the innate immune response. Curr Opin Immunol. 12(1), 13–9 (2000). [PubMed: 10679407]

6. Sampath V. et al. Altered postnatal lung development in C3H/HeJ mice. Pediatr Res. 60(6):663–8 (2006). [PubMed: 17065580]

7. Menden HL et al. Nicotinamide adenine dinucleotide phosphate oxidase 2 regulates LPS-induced inflammation and alveolar remodeling in the developing lung. Am J Respir Cell Mol Biol. 55(6), 767–778 (2016). [PubMed: 27438994]

8. Menden H. et al. Histone deacetylase 6 regulates endothelial MyD88-dependent canonical TLR signaling, lung inflammation, and alveolar remodeling in the developing lung. Am J Physiol Lung Cell Mol Physiol. 317(3), L332–L346 (2019). [PubMed: 31268348]

9. Korhonen EA et al. Tie1 controls angiopoietin function in vascular remodeling and inflammation. J Clin Invest. 126, 3495–510 (2016). [PubMed: 27548530]

10. Fukuhara S. et al. Differential function of Tie2 at cell-cell contacts and cell-substratum contacts regulated by angiopoietin-1. Nat Cell Biol. 10, 513–26 (2008). [PubMed: 18425120]

11. Brindle NP, Saharinen P, Alitalo K. Signaling and functions of angiopoietin-1 in vascular protection. Circ Res. 98, 1014–23 (2006). [PubMed: 16645151]

12. Hughes DP, Marron MB, Brindle NP The anti-inflammatory endothelial tyrosine kinase Tie2 interacts with a novel nuclear factor-kappaB inhibitor ABIN-2. Circ Res. 92(6), 630–6 (2003). [PubMed: 12609966]

13. Kim I. et al. Angiopoietin-1 regulates endothelial cell survival through the phosphatidylinositol 3'-Kinase/Akt signal transduction pathway. Circ Res. 86(1), 24–9 (2000). [PubMed: 10625301]

14. Scharpfenecker M, Fiedler U, Reiss Y, Augustin HG The Tie-2 ligand angiopoietin-2 destabilizes quiescent endothelium through an internal autocrine loop mechanism. J Cell Sci. 118(Pt 4), 771–80 (2005). [PubMed: 15687104]

15. Kim M. et al. Opposing actions of angiopoietin-2 on Tie2 signaling and FOXO1 activation. J Clin Invest. 126(9), 3511–25 (2016). [PubMed: 27548529]

16. Leligdowicz A, Richard-Greenblatt M, Wright J, Crowley VM, Kain KC Endothelial activation: the Ang/Tie axis in sepsis. Front Immunol. 9, 838 (2018). [PubMed: 29740443]

17. Wright JK et al. Biomarkers of endothelial dysfunction predict sepsis mortality in young infants: a matched case-control study. BMC Pediatr. 18(1), 118 (2018). [PubMed: 29571293]

18. Kümpers P. et al. Time course of angiopoietin-2 release during experimental human endotoxemia and sepsis. Crit Care. 13(3), R64 (2009). [PubMed: 19416526]

19. Hato T. et al. Angiopoietins contribute to lung development by regulating pulmonary vascular network formation. Biochem Biophys Res Commun. 381(2), 218–23 (2009). [PubMed: 19217887]

20. Huppert LA, Matthay MA, Ware LB Pathogenesis of acute respiratory distress syndrome. Semin Respir Crit Care Med. 40(1), 31–39 (2019) [PubMed: 31060086]

21. Ying L, Alvira CM, Cornfield DN Developmental differences in focal adhesion kinase expression modulate pulmonary endothelial barrier function in response to inflammation. Am J Physiol Lung Cell Mol Physiol. 315(1), L66–L77 (2018). [PubMed: 29597831]

22. Mei SH et al. Prevention of LPS-induced acute lung injury in mice by mesenchymal stem cells overexpressing angiopoietin 1. PLoS Med. 4(9), e269 (2007). [PubMed: 17803352]

23. David S, Mukherjee A, Ghosh CC et al. Angiopoietin-2 may contribute to multiple organ dysfunction and death in sepsis. Crit Care Med. 40(11), 3034–3041 (2012). [PubMed: 22890252]

24. Pfaffl MW A new mathematical model for relative quantification in real-time RT-PCR. Nucleic Acids Res. 29, e45 (2001).

25. Florence JM, Krupa A, Booshehri LM, Gajewski AL, Kurdowska AK Disrupting the Btk pathway suppresses COPD-like lung alterations in atherosclerosis prone ApoE(−/−) mice following regular exposure to cigarette smoke. Int J Mol Sci 19(2), E343 (2018). [PubMed: 29364178]

26. Knudsen L, Weibel ER, Gundersen HJG, Weinstein FV, Ochs M. Assessment of air space size characteristics by intercept (chord) measurement: an accurate and efficient stereological approach. J Appl Physiol. 108, 412–421 (2010). [PubMed: 19959763]

27. Cooney TP, Thurlbeck WM The radial alveolar count method of Emery and Mithal: a reappraisal 2–intrauterine and early postnatal lung growth. Thorax. 37, 580–583 (1982). [PubMed: 7179186]

28. Lignelli E, Palumbo F, Myti D, Morty RE Recent advances in our understanding of the mechanisms of lung alveolarization and bronchopulmonary dysplasia. Am J Physiol Lung Cell Mol Physiol. 317(6), L832–L887 (2019). [PubMed: 31596603]

29. Thébaud B, Abman SH Bronchopulmonary dysplasia: where have all the vessels gone? Roles of angiogenic growth factors in chronic lung disease. Am J Respir Crit Care Med. 175(10), 978–85 (2007). [PubMed: 17272782]

30. Mofarrahi M. et al. Regulation of angiopoietin expression by bacterial lipopolysaccharide. Am J Physiol Lung Cell Mol Physiol. 294(5), L955–63 (2008). [PubMed: 18310225]

31. McCarter SD et al. Cell-based angiopoietin-1 gene therapy for acute lung injury. Am J Respir Crit Care Med. 175(10), 1014–26 (2007). [PubMed: 17322110]

32. Witzenbichler B. et al. Protective role of angiopoietin-1 in endotoxic shock. Circulation. 111(1), 97–105 (2005). [PubMed: 15611372]

33. David S. et al. Acute administration of recombinant Angiopoietin-1 ameliorates multiple-organ dysfunction syndrome and improves survival in murine sepsis. Cytokine. 55(2), 251–9 (2011). [PubMed: 21531574]

34. Hegeman MA et al. Angiopoietin-1 treatment reduces inflammation but does not prevent ventilator-induced lung injury. PLoS One. 5(12), e15653 (2010).

35. Phanthanawiboon S. et al. Acute systemic infection with dengue virus leads to vascular leakage and death through tumor necrosis factor-α and Tie2/Angiopoietin signaling in mice lacking type I and II interferon receptors. PLoS One. 11(2), e0148564 (2016).

36. Iosef C. et al. Inhibiting NF-κB in the developing lung disrupts angiogenesis and alveolarization. Am J Physiol Lung Cell Mol Physiol. 302(10):L1023–36 (2012). [PubMed: 22367785]

37. McKenna S, Butler B, Jatana L, Ghosh S, Wright CJ Inhibition of IκBβ/NFκB signaling prevents LPS-induced IL1β expression without increasing apoptosis in the developing mouse lung. Pediatr Res. 82(6):1064–1072 (2017). [PubMed: 28753596]

38. Hakanpaa L. et al. Endothelial destabilization by angiopoietin-2 via integrin β1 activation. Nat Commun. 6, 5962 (2015). [PubMed: 25635707]

39. Thomas W. et al. Airway angiopoietin-2 in ventilated very preterm infants: association with prenatal factors and neonatal outcome. Pediatr Pulmonol. 46(8), 777–84 (2011). [PubMed: 21337734]

40. Thomas W. et al. Airway concentrations of angiopoietin-1 and endostatin in ventilated extremely premature infants are decreased after funisitis and unbalanced with bronchopulmonary dysplasia/death. Pediatr Res. 65(4), 468–73 (2009). [PubMed: 19127216]

41. Houghton AM Matrix metalloproteinases in destructive lung disease. Matrix Biol. 44–46, 167–74 (2015). [PubMed: 25686691]

42. Shrestha AK et al. Consequences of early postnatal lipopolysaccharide exposure on developing lungs in mice. Am J Physiol Lung Cell Mol Physiol. 316(1), L229–L244 (2019). [PubMed: 30307313]

43. Bhandari V. et al. Hyperoxia causes angiopoietin 2-mediated acute lung injury and necrotic cell death. Nat Med. 12(11), 1286–1293 (2006). [PubMed: 17086189]

44. Liang F, Zhu JX, Xia HP, Li HP, Zhu LC Effects of hyperoxia on lung vascular development and expression of angiopoietin-1 in neonatal rat lungs. Chin J Pediatr. 49(11), 834–8 (2011).

Impact statement:

- Key message: Angiopoietin 1 inhibits LPS-induced neonatal lung injury and alveolarremodeling

- Additions to existing literature:

  – Demonstrates dysregulation of angiopoietin-TIE2 axis is important for sepsis- induced acute lung injury and alveolar simplification in experimental BPD

  – Establishes recombinant Angiopoietin 1 as an anti-inflammatory therapy in BPD

- Impact: Angiopoietin 1-based interventions may represent novel therapies for mitigating sepsis-induced lung injury and BPD in premature infants
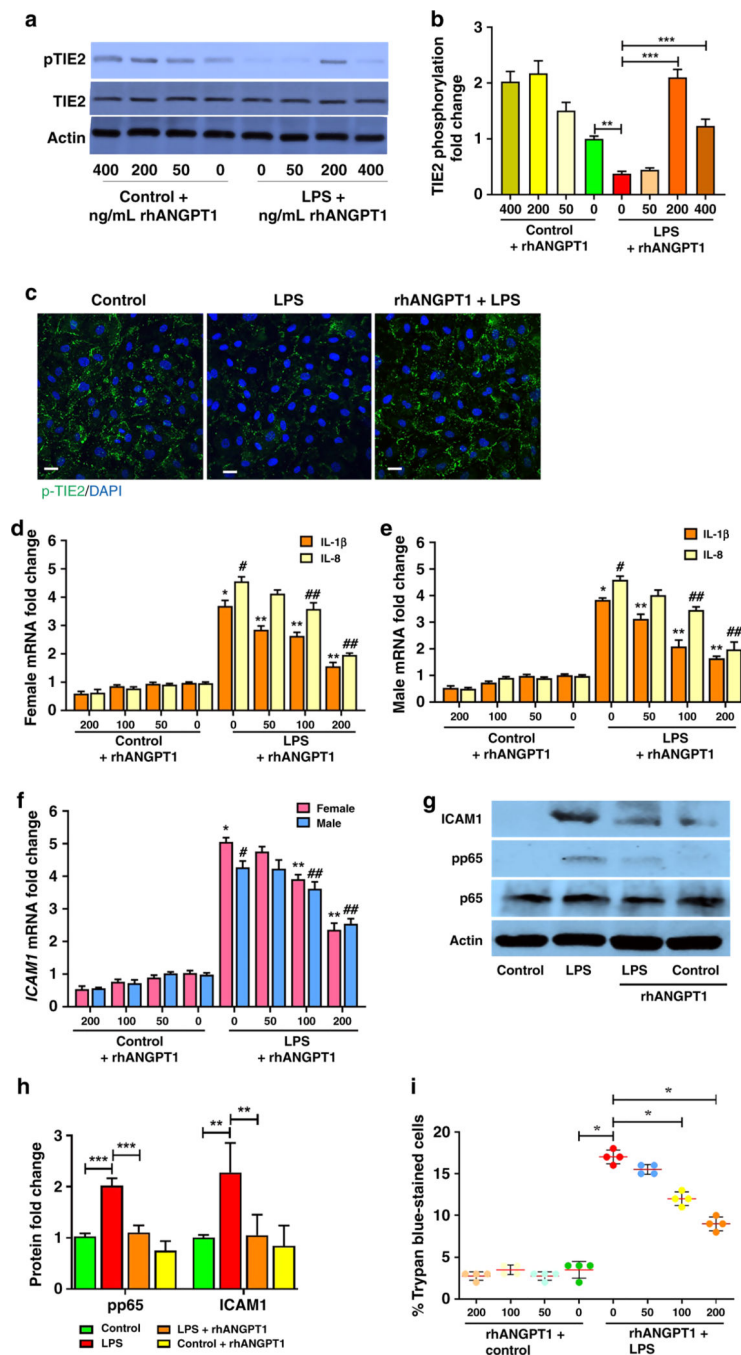
Figure 1–. LPS-induced EC activation is suppressed with rhANGPT1 in HPMEC.

(A) HPMEC in culture were treated with LPS (100ng/mL) and rhANGPT1 pre-treatment (1h) at different doses and lysates used for western blotting pTIE2, with quantification by densitometry **(B)**. (n=4/condition, **p<0.01; **p<0.001 between Control and LPS; LPS and LPS+rhANGPT1.) **(C)** HPMEC grown on coverslips were pre-treated with rhANGPT1 (500ng/mL for 1h) followed by LPS (100ng/mL) for 18h, and then used for pTIE2 (Green) and DAPI (nucleus) immunofluorescence. Scale bar indicates 10μm. (n=3/condition.) **(D, E, F)** *IL-1β, IL-8, and ICAM1* RNA expression was quantified

by RT-PCR in male and female HPMEC lysates treated with rhANGPT1 followed by LPS (100ng/mL) for 18h (n=3/sex/condition). (**D and E**); *p<0.001, **p<0.01 between Control vs. LPS, LPS vs. LPS+rhANGPT1 (*IL-1β*); #p<0.001, ##p<0.01 between Control vs. LPS, LPS vs. LPS+rhANGPT1 (*IL-8*). (**F**) *p<0.001, **p<0.01 between -Control vs. LPS, LPS vs. LPS+rhANGPT1 (Male); #p<0.001, ##p<0.05 between Control vs. LPS, LPS vs. LPS+rhANGPT1 (Female). (**G**) Immunoblots of ICAM1 and phosphorylated p65 protein from cell lysates 24h post-treatments, with densitometry shown (**H**). (n=4/condition, **p<0.01, ***p<0.001 between Control and LPS; LPS and LPS+rhANGPT1). ANOVA with post-hoc Tukey or Mann Whitney tests were used. (**I**) Cell viability by trypan blue assay. x axis denotes rhANGPT1 dose. (n=4/condition, *p<0.05 between Control and LPS; LPS and LPS+rhANGPT1 100 ng/mL; LPS and rhANGPT1 200 ng/mL).
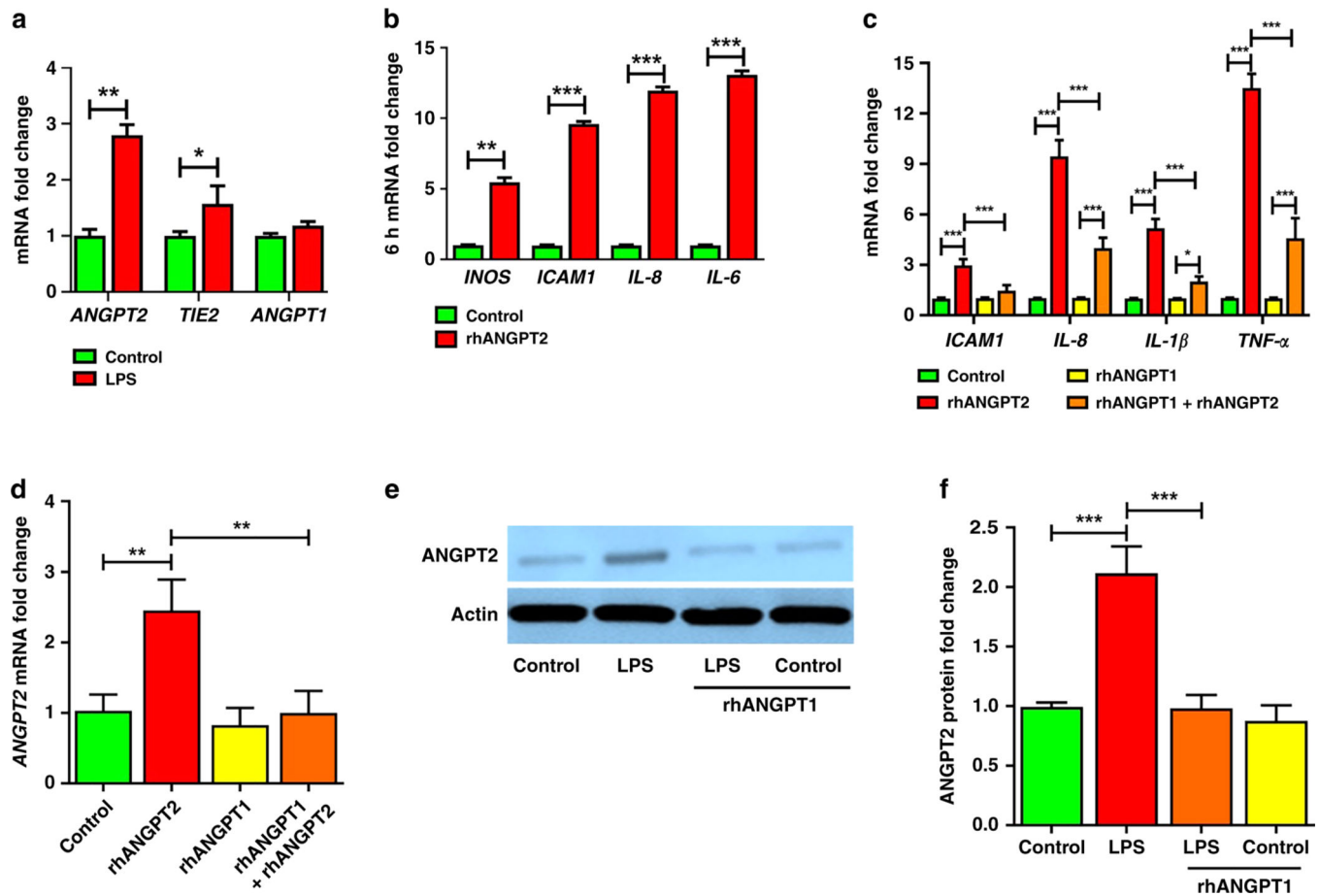
Figure 2–. ANGPT2 is upregulated by LPS in HPMEC and directly mediates EC immune activation, which is attenuated by rhANGPT1.
HPMEC were treated with LPS (100ng/mL), recombinant human ANGPT2 (rhANGPT2, 25ng/mL), and rhANGPT1 (200ng/mL), with lysates used for assays. **(A)** *ANGPT1*, *ANGPT2*, and *TIE2* gene expression by qPCR 24h after LPS. (n=4/condition, *p<0.05, **p<0.01.) **(B)** Quantification of *INOS*, *ICAM1*, *IL-8*, and *IL-6* expression by qPCR 6h after rhANGPT2. (n=4/condition, **p<0.01, ***p<0.001.) **(C-D)** HPMEC were treated for 24h with rhANGPT1 and rhANGPT2, and lysates were used to quantify gene expression of *IL-1β*, *ICAM1*, *IL-8*, and *TNF-α* **(C)** and *ANGPT2* **(D)** by qRT-PCR. (n=3/condition, *p<0.05, **p<0.01, ***p<0.001 between Control and rhANGPT2; rhANGPT2 and rhANGPT1+rhANGPT2; rhANGPT1 and rhANGPT1+rhANGPT2.) **(E)** ANGPT2 protein was quantified by immunoblot of HPMEC lysates 24h after rhANGPT1 and rhANGPT2 treatments, with densitometry shown **(F)**. (n=4/condition, ***p<0.001 between Control and LPS; LPS and LPS+rhANGPT1). ANOVA (with Tukey) or Mann Whitney tests were used.
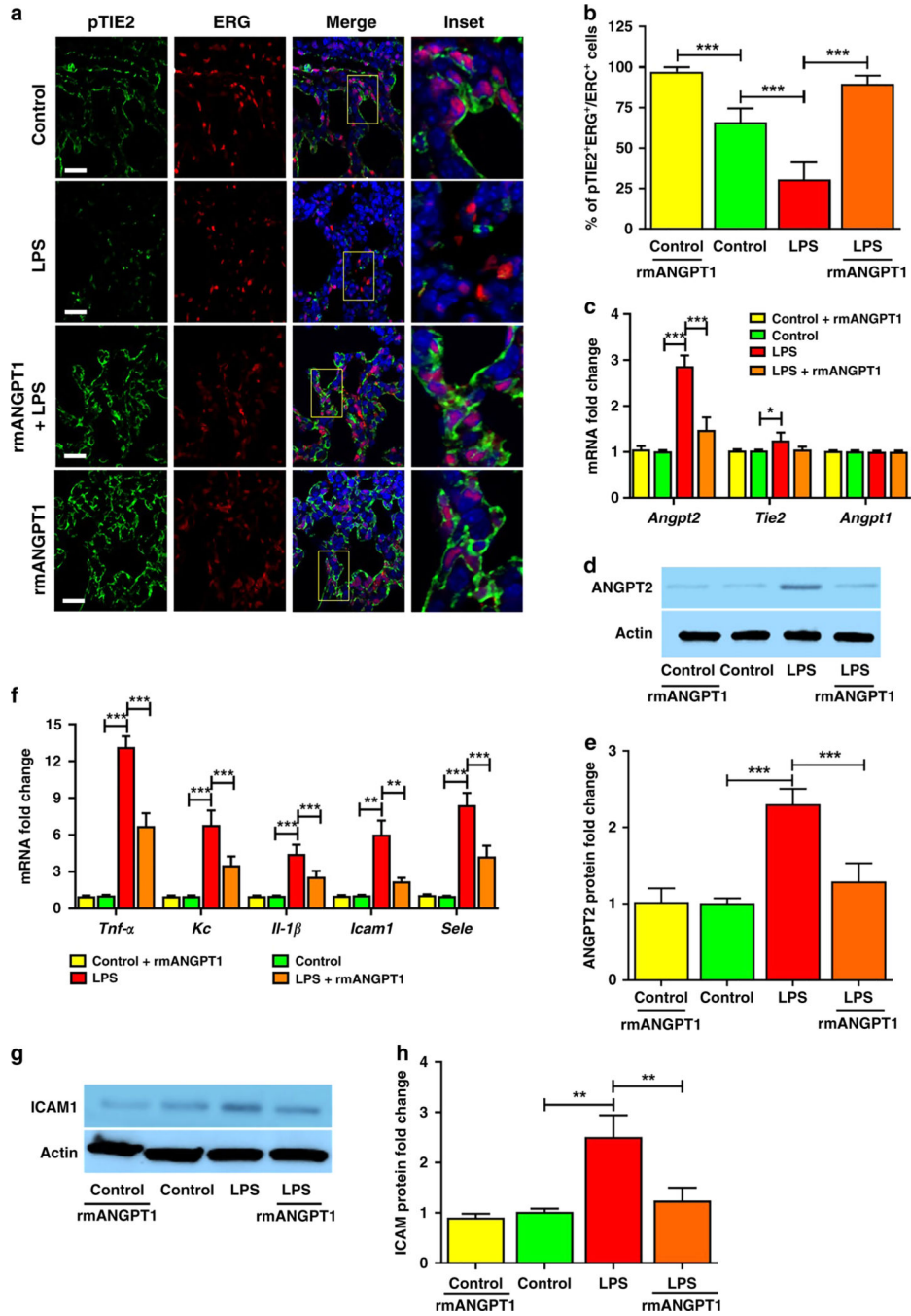
Figure 3–. rmANGPT1 restores TIE2 phosphorylation (pTIE2) and suppresses LPS-induced ANGPT2 and inflammation in mice

6-day-old mice were pre-treated with i.p rmANGPT1 (1μg, 2h), followed by vehicle or LPS (2mg/kg i.p). Lung sections or homogenates obtained after 24h were used for assays. **(A)** Immunofluorescent staining for pTIE2 (green), ERG (red), and DAPI (blue) in lung sections, with quantification of pTIE2+:ERG+ co-staining per high power field (HPF) shown **(B)**. Scale bar indicates 10μm. (n 5/condition, ***p<0.001 between Control and Control+rmANGPT1; Control and LPS; LPS and LPS+rmANGPT1.) **(C)** Whole

lung gene expression of *Angpt2*, *Angpt1*, and *Tie2* by qPCR. (n=5/condition, (*p<0.05, ***p<0.001 between Control and LPS; LPS and LPS+rmANGPT1.) **(D)** ANGPT2 protein by immunoblot, with quantification by densitometry shown **(E)**. (n 5/condition, ***p<0.001 between Control and LPS; LPS and LPS+rmANGPT1.) **(F)** *Tnf-a*, *Il-1β*, *Kc* (*IL-8*), *Icam1*, and *Sele* (E-selectin) RNA expression was quantified by qPCR. (n=5/condition, **p<0.01, ***p<0.001 between Control and LPS; LPS and LPS+rmANGPT1.) **(G)** ICAM1 protein was quantified by immunoblot, with densitometry shown graphically **(H)**. (n 5/condition, **p<0.01 between Control and LPS; LPS and LPS+rmANGPT1.) ANOVA (with Tukey) or Mann Whitney tests were used.
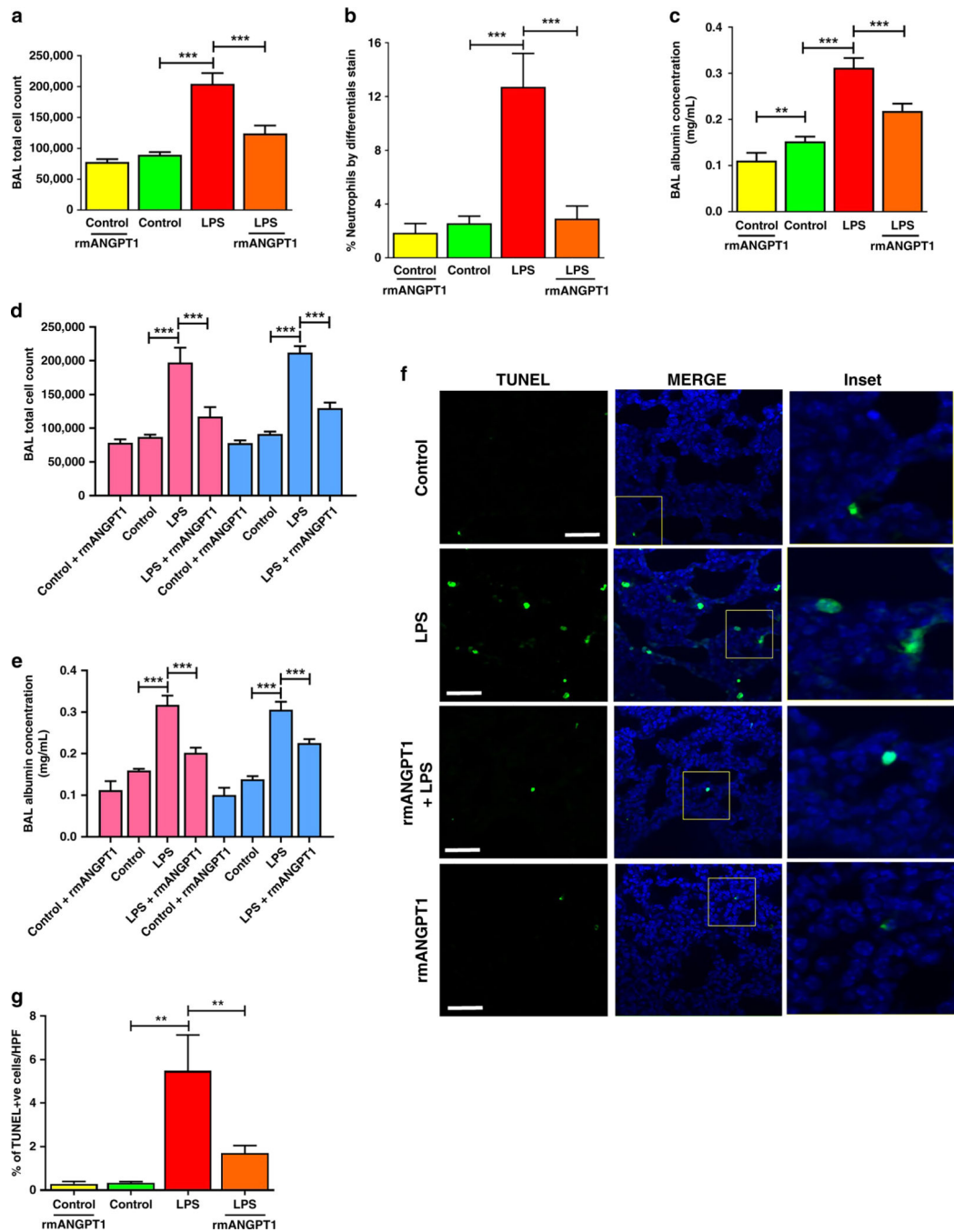
Figure 4–. Acute lung injury is attenuated by rmANGPT1 in LPS-treated mice.

(A-C) Bronchoalveolar lavage (BAL) was performed on 11-day-old mice 24h after treatments with LPS (2mg/kg i.p) and 2h rmANGPT1 pre-treatment. Lavage fluid was used for: Total cell counts **(A)**; Neutrophil quantification **(B)**; Protein concentration **(C)** with quantifications shown graphically. (n 5/condition, **p<0.01, ***p<0.001 between Control and LPS; LPS and LPS+rmANGPT1; Control and Control+rmANGPT1.) **(D-E)** BAL total cell counts and albumin concentrations were analyzed by sex. Pink bars represent females and blue bars represent males. (n 3/condition, ***p<0.001 between Control and

LPS; LPS and LPS+rmANGPT1.) **(F)** 7-day-old mice treated with LPS, with or without rmANGPT1, were used to obtain lung tissue sections for TUNEL (green) and DAPI (blue) immunofluorescence. Scale bar indicates 50μm. **(G)** Graphical representation summarizing the ratio of TUNEL+ to total cell count per HPF. (n=5/condition, **p<0.01 between Control and LPS; LPS and LPS+rmANGPT1.) ANOVA (post-hoc Tukey) or Mann Whitney tests were used.
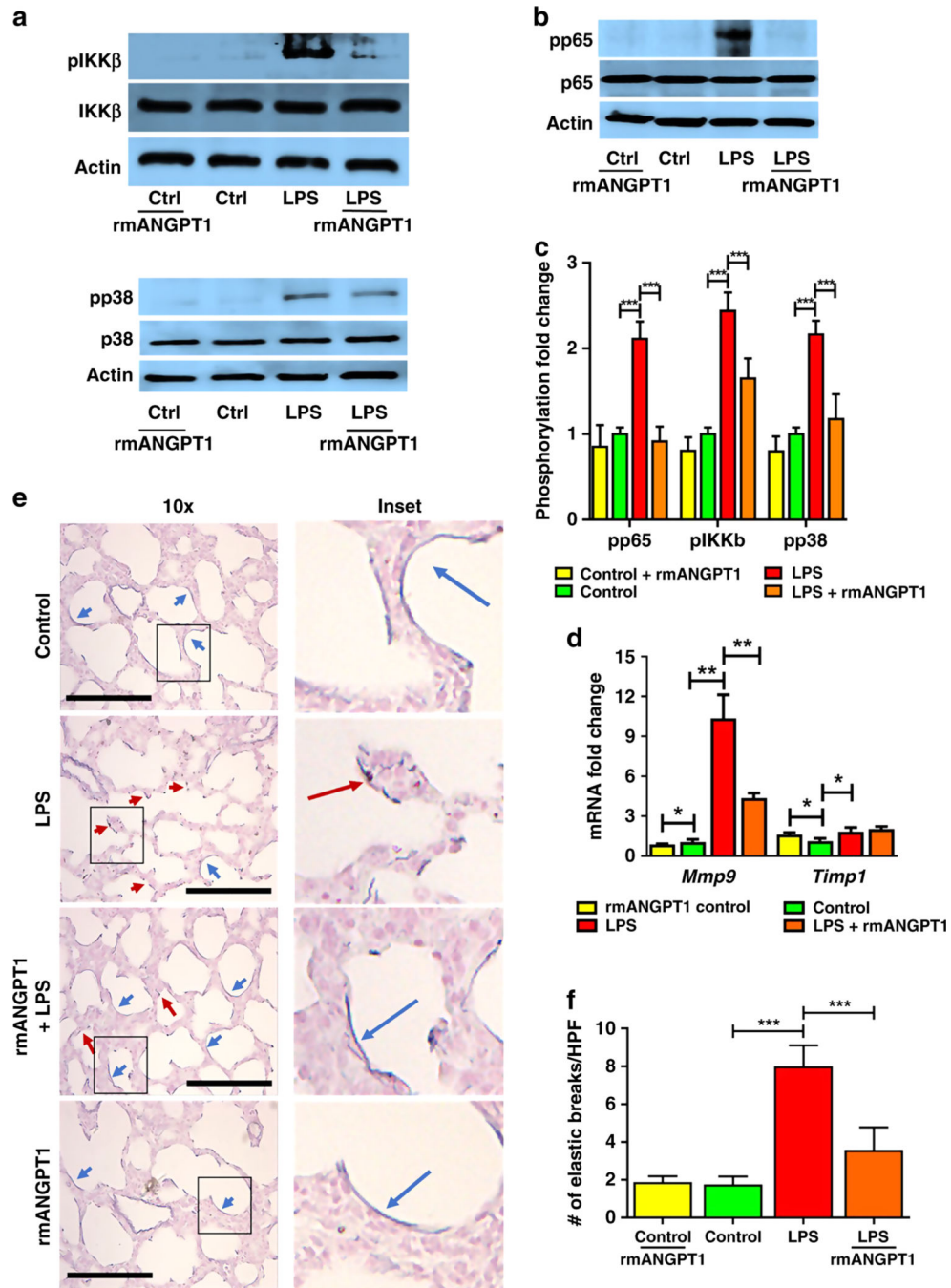
Figure 5–. rmANGPT1 modifies TLR4 signaling and matrix degradation during sepsis in mice.
6-day-old pups were injected with LPS and rmANGPT1 pre-treatment, and lungs were
harvested 24h post-treatment for assays and staining. **(A-C)** Lung homogenates were used
to quantify the phosphorylation of IKKb and p38 **(A)**, and p65 **(B)** by immunoblotting,
with densitometry shown **(C)**. (n=5/condition, ***p<0.001 between Control and LPS;
LPS and LPS+rmANGPT1.) **(D)** *Mmp9* and *Timp1 gene* expression by qPCR from
lung homogenates. (n=5/condition, *p<0.05, **p<0.01 between Control and LPS; LPS
and LPS+rmANGPT1; Control and Control+rmANGPT1.) **(E)** Lung tissue sections were

assessed for elastic fiber structure (blue) using Resorcin-Fuchsin staining with Carmine counter stain, with disrupted elastic fibers shown by red arrows and continuous fibers shown by blue arrows. Scale bar indicates 30μm. **(F)** Quantification of elastic fiber breaks/HPF, is shown. (n=5/condition, ***p<0.001 between Control and LPS; LPS and LPS+rmANGPT1.) ANOVA (post-hoc Tukey tests) or Mann Whitney tests were used.
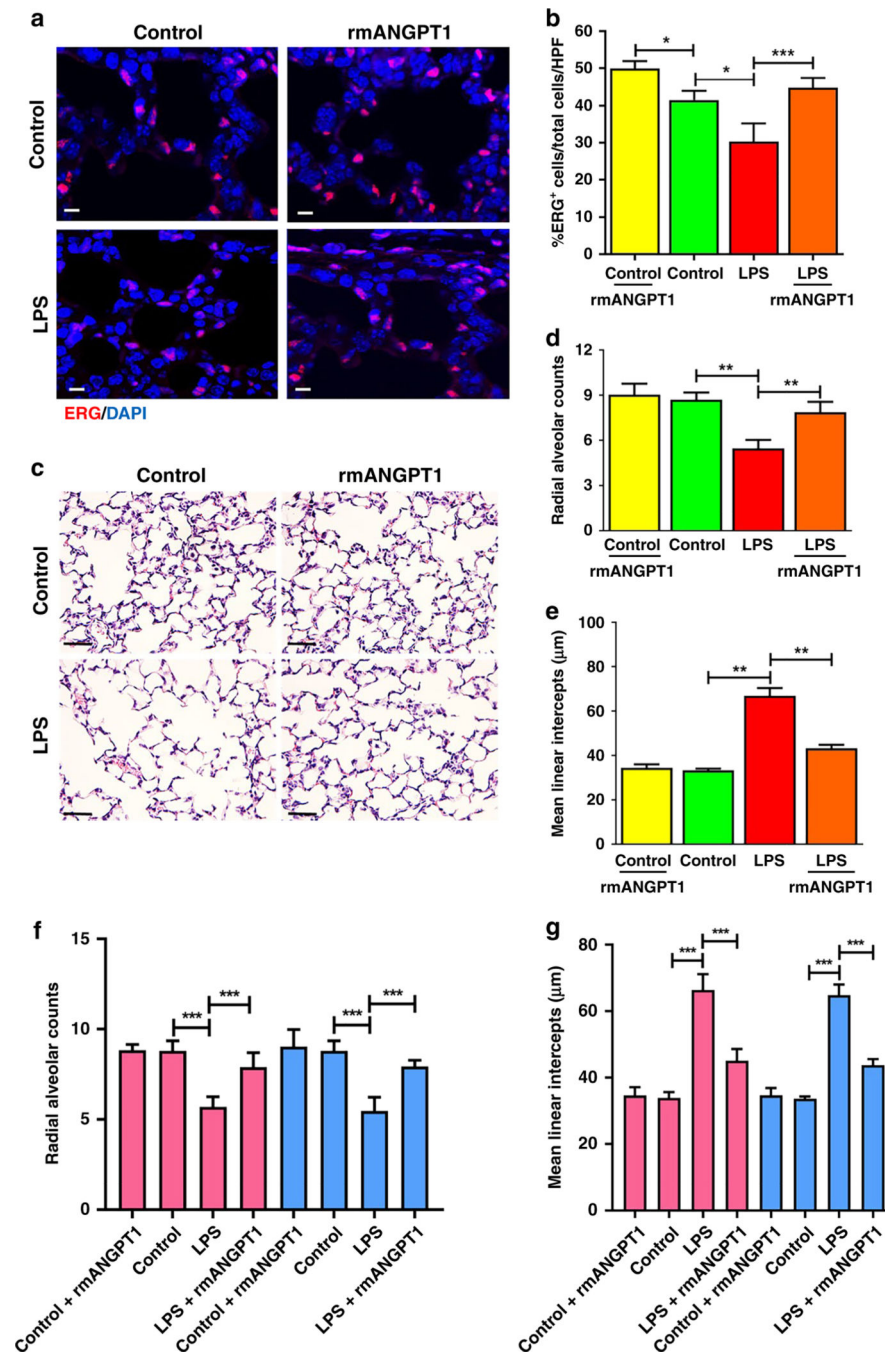
Figure 6–. Effect of rmANGPT1 on LPS-induced long-term lung growth and remodeling in mice.
Sections of formalin-inflated lungs from 15-day-old mice, 196h post-LPS treatment, with or without rmANGT1 treatments (one dose 2h prior to LPS and another 72h after LPS) were stained. **(A)** Immunofluorescent staining of ERG (red) and DAPI (blue), with quantification of ERG+/Total cells/HPF shown **(B)**. Scale bar indicates 10μm. (n 5/ condition, *p<0.05, ***p<0.001 between Control and LPS; LPS and LPS+rmANGPT1; Control and Control+rmANGPT1.) **(C-E)** H&E staining **(C)** used to quantify radial alveolar counts **(D)** and mean linear intercepts **(E)**. Scale bar indicates 50μm. (n 5/condition,

p<0.01 between Control and LPS; LPS and LPS+rmANGPT1.) **(F) and **(G)** Radial alveolar counts and mean linear intercepts were further analyzed by mouse sex. Pink bars represent females and blue bars represent males. (n 3/condition, ***p<0.001 between Control and LPS; LPS and LPS+rmANGPT1). ANOVA with Tukey tests were used.